

monomer-dominated emission (P_1) or a triplet excimer (P_2) (Fig. 1)?

After an overview of previous reports concerning purely organic RTP, it was found that the RTP was more likely to be monomer-dominated emission (P_1), as just the corresponding monomer-dominated fluorescence (F_1) occurred and no excimer fluorescence (F_2) could be observed.^{1–4} However, there has been no direct and powerful proof to confirm this point, for the lack of appropriate RTP examples. As mentioned above, the π - π stacking in molecular dimers could lead to the persistent RTP effect in phenothiazine 5,5-dioxide derivatives, and also a singlet excimer could be formed as a result of π - π interactions in some cases.⁵ Thus, persistent RTP and singlet excimer emission (F_2) could be integrated together, with suitable intermolecular π - π interactions. Then, through a careful comparison of emission peaks between RTP and singlet excimer, the above questions might be answered, as the triplet state is always lower in energy than the corresponding singlet one in theory. Besides, to well distinguish RTP from monomer-dominated emission or a triplet excimer, a small energy gap (ΔE_{ST}) between excited singlet (S_1) and triplet (T_1) states should be necessary. With this, the fluorescence and phosphorescence could closely appear in pairs (F_1/P_1 and F_2/P_2). Thus, thermally activated delayed fluorescence (TADF) luminogens with minimized energy gap between S_1 and T_1 states would be a good choice.⁶

In order to realize integrated RTP, with singlet excimer and TADF effects in one luminogen, two RTP building blocks of phenothiazine 5,5-dioxide and dimethyl isophthalate were combined together through the twisted linkage mode of a C–N bond to yield CS-2COOCH₃.^{4d,e,7} With this structure, three main purposes could be achieved. Firstly, the persistent RTP effect could be maintained with the integration of two simple RTP building blocks. Secondly, the small ΔE_{ST} , as well as the TADF effect, would be more likely to be realized with this twisted D–A structure, in which the phenothiazine 5,5-dioxide group acted as electron donor (D) and dimethyl isophthalate as acceptor (A). Thirdly, the planar conformations of donor and acceptor units could promote multiple intermolecular π - π interactions, thus allowing realization of the formation of an excimer. Fortunately, persistent RTP and singlet excimer emissions, as well as the TADF effect, were all integrated into the target compound CS-2COOCH₃, just as expected. With this, in-depth analyses of the excited state process in RTP became possible. And it was found that the persistent RTP was monomer dominated (P_1), rather than from a triplet excimer (P_2).

Results and discussion

CS-2COOCH₃ could be easily synthesized through carbon-nitrogen coupling reaction, followed by oxidation with hydrogen peroxide (Scheme S1†). The molecular structure and purity have been well determined by ¹H and ¹³C NMR spectra, high-resolution mass spectrum, elemental analysis and high-performance liquid chromatography. A crystal of CS-2COOCH₃ showed the expected persistent RTP effect, and its afterglow could last for more than 1 s after turning off 365 nm UV

radiation. However, it was strange that the afterglow was much blue-shifted compared to the one under UV irradiation (Fig. 2). This was totally different from the common RTP phenomena in previous reports, as the excited triplet state should be lower in energy than the corresponding singlet one in theory.¹ Then photoluminescence (PL) spectra of a crystal, including fluorescence and phosphorescence, were measured at room temperature under air or N₂ atmosphere (Fig. 2 and S1†). As shown in Fig. 2A and C, two very different emission peaks at 405 and 505 nm appeared in the fluorescence spectrum, while the main peak of RTP was located at 430 nm, accompanied by two shoulder peaks at 460 and 490 nm. The same went for those under N₂ atmosphere (Fig. S1†). All of the three phosphorescence peaks showed similar excitation spectra, indicating the shoulder peaks came from the vibration energy levels of the main phosphorescence one (Fig. S2†). Thus, the occurrence of long-wavelength fluorescence around 505 nm should be the main reason for the visual blue-shifted afterglow. Then why did the CS-2COOCH₃ crystal show double fluorescence emissions?

In order to clarify this, CS-2COOCH₃ was doped in poly(methyl methacrylate) (PMMA) with a mass fraction of about 5% or dissolved in tetrahydrofuran (THF) to eliminate the influence of intermolecular interactions. As shown in Fig. 2A, C and in S3,† there was just one fluorescence peak at around 420 nm and no phosphorescence peak for the doped film and THF solution, in which the intermolecular interactions could be diminished and the emission was only from the monomer. Thus, the corresponding short-wavelength fluorescence peak at 405 nm for

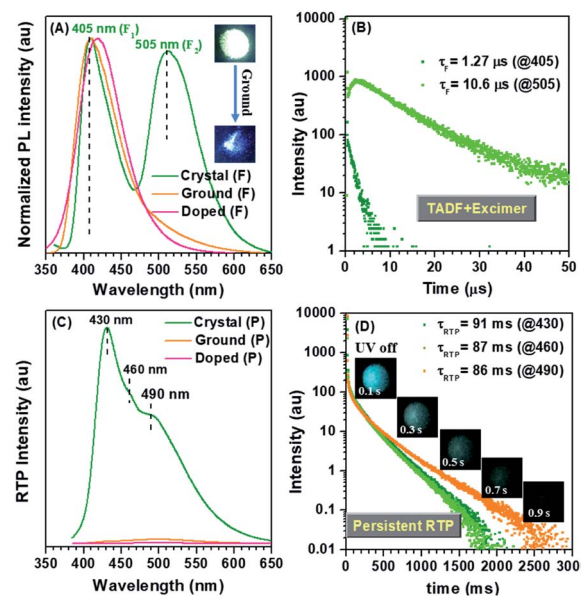


Fig. 2 (A) The normalized steady-state PL spectra of CS-2COOCH₃ in different states—crystal, ground state and doped in poly(methyl methacrylate) (PMMA) film in air. (B) The fluorescence decay curves of CS-2COOCH₃ crystal at 405 and 505 nm in air. (C) The RTP spectra, acquired after 10 ms delay, of CS-2COOCH₃ in different states—crystal, ground state and doped in PMMA film under air atmosphere. (D) The RTP decay curves of CS-2COOCH₃ crystal at 430, 460 and 490 nm. Insets: photos of CS-2COOCH₃ crystal before and after turning off 365 nm UV radiation in air.



the crystal should be also monomer-dominated emission (F_1), while the one at 505 nm was from aggregates, such as singlet excimer (F_2).

To further confirm this point, the UV-visible absorption spectra of CS-2COOCH₃ in different states were measured. As shown in Fig. S4,† one more shoulder peak at long wavelength of about 365 nm could be observed for CS-2COOCH₃ crystal, while this peak disappeared in the solution state. This indicated the strong intermolecular coupling in the crystal. After it was ground heavily, the shoulder peak at 365 nm weakened largely, accompanied by nearly disappearing excimer emission at 505 nm, as a result of the destruction of molecular packing (Fig. S4† and 2A). Also, the excitation spectra of the two fluorescence peaks in the crystal were similar, which were both red-shifted in comparison with that in the solution state (Fig. S5†). These could well demonstrate the formation of a singlet excimer in the crystal with a particular molecular packing mode.⁸ Also, powder X-ray diffraction (PXRD) was carried out to monitor the molecular packing in the crystal and ground states of CS-2COOCH₃. As shown in Fig. S6,† the PXRD pattern of the CS-2COOCH₃ crystal was similar to the computed XRD pattern (as derived from X-ray crystallography), which could rule out the possible presence of two crystalline morphologies. After it was ground heavily, the PXRD peaks nearly disappeared as a result of the destroyed molecular packing. At the same time, the PL spectrum and corresponding excitation spectrum in the ground state were similar to those for the doped film (Fig. S7†), while their PL lifetimes were much different (Fig. S8†). It was believed that the rigid environment from PMMA could decrease the non-radiative motion of CS-2COOCH₃ and restrict the diffusion of oxygen, thus leading to the much longer emission lifetime in PMMA film. Besides, the crystal and doped PMMA film of CS-2COOCH₃ showed a similar TADF effect for their short-wavelength emissions at 405 or 420 nm with average lifetimes (τ_{FS}) of about 1 μ s, while the one at 505 nm was much longer (10.6 μ s) (Table 1). This could be well consistent with the character of a singlet excimer.⁸ On the other hand, an increasing component was observed in the time-resolved curve of 505 nm (Fig. 2B), which might come from its special PL process in the excited state. According to these experimental results, it was confirmed that the 505 nm emission in the fluorescence spectrum was indeed from the singlet excimer (F_2), while the one at 405 nm was monomer-dominated emission (F_1).

Interestingly, a unique double TADF effect was observed for the CS-2COOCH₃ crystal in both monomer-dominated emission (F_1) and excimer emission (F_2) (Fig. 2B). To the best of our

knowledge, this is the first example of double TADF effects in both monomer-dominated emission and excimer emission.⁹ Besides, the ΔE_{ST} of the crystal was measured to be only about 0.17 eV according to the low-temperature (77 K) PL spectra (Fig. S9†), which should be small enough to allow the inter-system crossing between S_1 and T_1 states, and thus to lead to the TADF effect. Then the temperature-dependent PL spectra of the CS-2COOCH₃ crystal were measured from 77 K to room temperature. As shown in Fig. 3, the fluorescence peaks at 386 and 495 nm were much lower than those of phosphorescence (407 and 430 nm) at 77 K. With increasing temperature, the ratios of fluorescence peaks both increased, while those of phosphorescence decreased. At last, just two fluorescence peaks at about 405 and 505 nm could be observed at room temperature, and those of phosphorescence were much weakened. Since the TADF effect should be promoted with the increased temperature, these experimental results could well confirm the emission peak at 505 nm as the thermally activated delayed singlet excimer emission, rather than phosphorescence. Also, because of this unique TADF effect, the monomer-dominated fluorescence (F_1) (405 nm) and phosphorescence (P_1) (430 nm) could closely appear in pairs, just as we expected. Thus, the ideal PL spectra were achieved to identify the role of molecular dimer in the persistent RTP effect. With this, it was easy to determine that the persistent RTP should be monomer-dominated emission (P_1), rather than triplet excimer emission (P_2).

To explore the internal mechanism, the single-crystal structure of CS-2COOCH₃ was carefully analyzed (Table S1†). As shown in Fig. 4, CS-2COOCH₃ presented a twisted D-A conformation for the C-N linkage mode, which would be much



Fig. 3 Normalized PL spectra of CS-2COOCH₃ crystal from 77 K to 298 K.

Table 1 The lifetimes of CS-2COOCH₃ in different states ($\tau_F = A_1\tau_1 + A_2\tau_2$; A_1 : fraction of the shorter component; τ_1 : lifetime of the shorter component; A_2 : fraction of longer-lived component; τ_2 : lifetime of the longer component)

State	λ_F (nm)	τ_1 (ns)	A_1 (%)	τ_2	A_2 (%)	τ_F	Φ_F (%)	λ_P (nm)	τ_P (ms)
Solution	430	18.0	100	—	—	18.0 ns	21.82	—	—
Crystal	405	55.2	13.14	1.45 μ s	86.86	1.27 μ s	7.96	430/460/490	91/87/86
	505	10.0	3.74	11.0 μ s	96.26	10.6 μ s	—	—	—
Ground	410	19.3	73.39	61.47 ns	26.61	33.6 ns	15.58	—	—
Doped	420	30.0	56.36	2.20 μ s	43.64	0.97 μ s	10.40	—	—



beneficial for its TADF effect. Because of the planar conformations of phenothiazine 5,5-dioxide and dimethyl isophthalate units, they both presented parallel stacks facing each other in the crystal. Besides, the π - π vertical distance for adjacent phenothiazine 5,5-dioxide units was as short as 3.76 Å, while that of adjacent dimethyl isophthalate units was 3.59 Å, indicating the existence of multiple π - π interactions. With these, the unique molecular dimers were formed, thus allowing realization of singlet excimer emission. Furthermore, all of the molecular dimers were perpendicular or parallel to each other, which could well ensure the relatively strong singlet excimer emission at 505 nm. Also, with the effective π - π interactions, the persistent RTP effect could be achieved for the decreased phosphorescent radiative and non-radiative rates, just as in our previous reports.^{4d,e} Then why was the RTP a monomer-dominated emission, rather than from a triplet excimer?

To answer this question, the natural transition orbitals (NTOs) of the T_1 state for the monomer and dimer (derived from its single-crystal structure) of CS-2COOCH₃ were evaluated by time-dependent density functional theory calculation.¹⁰ As shown in Fig. 4B, both monomer and dimer gave a charge transfer (CT)-dominated T_1 state with hole located at phenothiazine 5,5-dioxide unit and particle mainly at dimethyl isophthalate unit. Particularly, only one molecule was involved in the NTO of the T_1 state for the molecular dimer, which should be the main reason for the monomer-dominated RTP emission of the CS-2COOCH₃ crystal. Besides, owing to the twisted D-A structure of CS-2COOCH₃, the well-separated HOMOs and LUMOs could be achieved in both the monomer and dimer of CS-2COOCH₃ (Fig. S10†). With this, a minimized ΔE_{ST} could be achieved, resulting in the TADF effect and close fluorescence/phosphorescence peaks. Thus, although molecular dimers existed in the crystal, the RTP from the excited triplet state was still monomer-dominated emission, rather than triplet excimer emission.

Then how did the monomer (involved in π - π stacking) generate persistent RTP? Actually, we could get some clues from

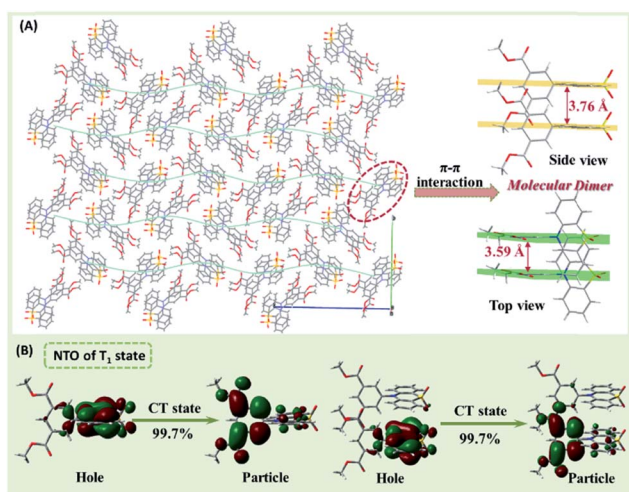


Fig. 4 (A) The single-crystal structure and molecular dimer (side view and top view) of CS-2COOCH₃. (B) The natural transition orbitals (NTOs) of the T_1 state for the monomer and dimer of CS-2COOCH₃.

the corresponding fluorescence properties. The fluorescent radiative rate (k_r) and non-radiative rate (k_{nr}) for CS-2COOCH₃ in different states were estimated based on the corresponding fluorescence lifetimes (τ) and quantum yields (Φ_F), including the doped PMMA film (@420 nm), monomer-dominated emission in the crystal (@405 nm) and excimer emission in the crystal (@505 nm) (Table S2†). Their changing tendency is summarized in Fig. 5. Among them, the molecules doped in PMMA gave the highest k_r and k_{nr} for the eliminated intermolecular interaction. As for the monomer involved in π - π stacking in the crystal, its k_r and k_{nr} (@405 nm) decreased, thus benefiting a prolonged fluorescence lifetime according to the equation of $\tau = 1/(k_r + k_{nr})$.^{4d,7a} Similarly, the lifetimes of triplet excitons could also be prolonged for the monomer involved in π - π interactions with much decreased phosphorescent radiative and non-radiative rates, thus resulting in the persistent RTP effect. As for the triplet state of the excimer, its phosphorescence radiative rate would be too slow to compete with the corresponding singlet one, and thus no emission could be realized for it.

As revealed by the experimental results, coupled with theoretical calculations, it could be concluded that the persistent RTP was monomer-dominated emission (P_1), rather than from a triplet excimer (P_2). Thus, the PL process in the excited state of CS-2COOCH₃ could be understood clearly (Fig. 6). First, monomers absorbed photons to form singlet excitons. Because of the small energy gap between S_1 and T_1 states, efficient intersystem crossing (ISC) and reverse intersystem crossing (RISC) between them could happen for some excitons, leading to the TADF emission with a lifetime of about 1 μ s. Subsequently, some of the singlet excitons could interact with adjacent molecules in the ground state to form singlet excimers, for which the emission lifetime would further increase to about 10 μ s for the decreased fluorescent radiative and non-radiative rates. On the other hand, some of the formed triplet excitons, originating from the ISC transition, would be trapped in T_1^* (mono) state with much decreased phosphorescent radiative and non-radiative rates for the π - π interactions. Finally, monomer-dominated persistent RTP occurred with lifetime up to about 90 ms. As for the triplet state of the excimer, no emission could be achieved for the ultra-low radiative rate.

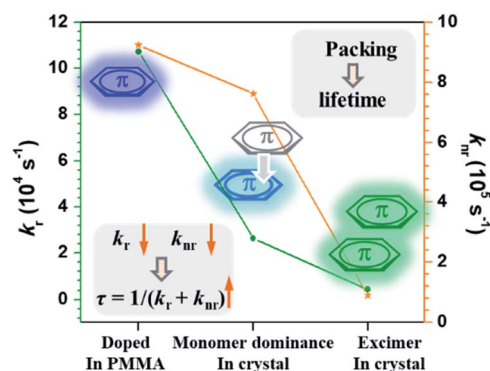


Fig. 5 Changing tendency of the fluorescent radiative rate (k_r) and non-radiative rate (k_{nr}) for CS-2COOCH₃ in different states.



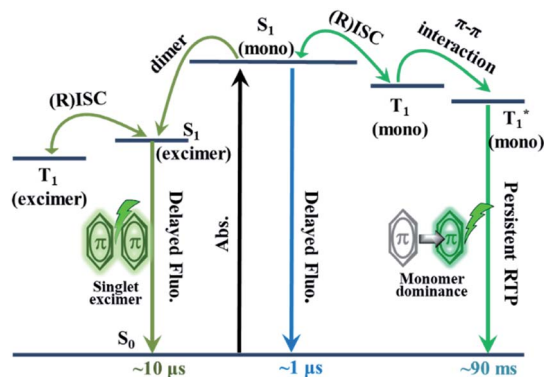


Fig. 6 The proposed PL process of CS-2COOCH₃.

Analyzing the PL process in Fig. 6 carefully, it was not difficult to find that the microsecond-scale component of the singlet excimer (@505 nm) could be promoted through two ways (1 and 2), while that of the nanosecond-scale one was just from one way (3):

(1) $S_0 \rightarrow S_1(\text{mono}) \rightarrow S_1(\text{excimer}) \rightarrow T_1(\text{excimer}) \rightarrow S_1(\text{excimer}) \rightarrow S_0$ (microsecond fluorescence);

(2) $S_0 \rightarrow S_1(\text{mono}) \rightarrow T_1(\text{mono}) \rightarrow S_1(\text{mono}) \rightarrow S_1(\text{excimer}) \rightarrow S_0$ (microsecond fluorescence);

(3) $S_0 \rightarrow S_1(\text{mono}) \rightarrow S_1(\text{excimer}) \rightarrow S_0$ (nanosecond fluorescence).

As additional microsecond-scale excitons could be formed through way (2) in the singlet excimer emission, in comparison with traditional TADF luminogens, an increasing component could be observed in the delayed component of 505 nm (Fig. 2B). Also, this could confirm the accuracy of the proposed PL process in Fig. 6 from another perspective.

Conclusions

In summary, the unique singlet excimer emission and TADF effect have been successfully integrated into the RTP luminogen of CS-2COOCH₃ for the first time. Furthermore, the excited-state process of RTP was revealed clearly with the aid of these unique effects, especially for the role of molecular dimers in the persistent RTP emission. In previous reports, molecular dimers were frequently found to play an important role in the RTP effect, but their specific working mechanism has not been revealed in detail or just been simulated by theoretical calculation. This work has made the first attempt to reveal the actual role of dimers in the RTP effect based on solid experimental results. Of note, the ideal target RTP luminogen with two other unique emission effects was obtained with both rational molecular design and good luck. Incorporating the excited-state characteristics of singlet excimer emission and TADF, it has been well demonstrated that the persistent RTP was monomer dominated, rather than from a triplet excimer. The information obtained from this study would be of great importance for gaining a clear and deep understanding of the whole RTP process, thus guiding the further development of this research area.

Conflicts of interest

There are no conflicts to declare.

Acknowledgements

We are grateful to the starting grants of Tianjin University and Tianjin Government, National Natural Science Foundation of China (no. 51903188) and Natural Science Foundation of Tianjin City (No. 19JCQNJC04500) for financial support.

Notes and references

- (a) R. Kabe and C. Adachi, *Nature*, 2017, **550**, 384–387; (b) S. Fatemina, Z. Mao, S. Xu, Z. Yang, Z. Chi and B. Liu, *Angew. Chem., Int. Ed.*, 2017, **56**, 12160–12164; (c) M. Fang, J. Yang, X. Xiang, Y. Xie, Y. Dong, Q. Peng, Q. Li and Z. Li, *Mater. Chem. Front.*, 2018, **2**, 2124–2129; (d) L. Huang, B. Chen, X. Zhang, C. Trindle, F. Liao, Y. Wang, H. Miao, Y. Luo and G. Zhang, *Angew. Chem., Int. Ed.*, 2018, **57**, 16046–16050; (e) C. A. M. Salla, G. Farias, M. Rouzières, P. Dechambenoit, F. Durola, H. Bock, B. d. Souza and I. H. Bechtold, *Angew. Chem., Int. Ed.*, 2019, **58**, 6982–6986; (f) S. Hirata, *Adv. Sci.*, 2019, **6**, 1900410; (g) K. Jinnai, R. Kabe and C. Adachi, *Adv. Mater.*, 2018, 1800365; (h) T. Ogoshi, H. Tsuchida, T. Kakuta, T. Yamagishi, A. Taema, T. Ono, M. Sugimoto and M. Mizuno, *Adv. Funct. Mater.*, 2018, 1707369; (i) Y. Shoji, Y. Iwabata, Q. Wang, D. Nemoto, A. Sakamoto, N. Tanaka, J. Seino, H. Nakai and T. Fukushima, *J. Am. Chem. Soc.*, 2017, **1397**, 2728–2733; (j) J. S. Ward, R. S. Nobuyasu, A. S. Batsanov, P. Data, A. P. Monkman, B. Dias and M. R. Bryce, *Chem. Commun.*, 2016, **52**, 2612–2615.
- (a) Kenry, C. Chen and B. Liu, *Nat. Commun.*, 2019, **10**, 2111; (b) X. Ma, J. Wang and H. Tian, *Acc. Chem. Res.*, 2019, **52**, 738–748; (c) S. Hirata, *Adv. Opt. Mater.*, 2017, 1700116.
- (a) J. Yang, Z. Ren, Z. Xie, Y. Liu, C. Wang, Y. Xie, Q. Peng, B. Xu, W. Tian, F. Zhang, Z. Chi, Q. Li and Z. Li, *Angew. Chem., Int. Ed.*, 2017, **56**, 880–884; (b) J. Yang, X. Gao, Z. Xie, Y. Gong, M. Fang, Q. Peng, Z. Chi and Z. Li, *Angew. Chem., Int. Ed.*, 2017, **56**, 15299–15303; (c) S. Cai, H. Shi, D. Tian, H. Ma, Z. Cheng, Q. Wu, M. Gu, L. Huang, Z. An, Q. Peng and W. Huang, *Adv. Funct. Mater.*, 2018, 1705045; (d) E. Lucenti, A. Forni, C. Botta, L. Carlucci, C. Giannini, D. Marinotto, A. Pavanello, A. Previtali, S. Righetto and E. Cariati, *Angew. Chem., Int. Ed.*, 2017, **56**, 16302–16307; (e) Q. Li, Y. Tang, W. Hu and Z. Li, *Small*, 2018, 1801560; (f) B. Zhou and D. Yan, *Adv. Funct. Mater.*, 2019, **29**, 1807599; (g) J. Yuan, S. Wang, Y. Ji, R. Chen, Q. Zhu, Y. Wang, C. Zheng, Y. Tao, Q. Fan and W. Huang, *Mater. Horiz.*, 2019, **6**, 1259–1264; (h) J. Yang, Z. Chi, W. Zhu, B. Tang and Z. Li, *Sci. China: Chem.*, 2019, **62**, 1090–1098; (i) M. Fang, J. Yang and Z. Li, *Chin. J. Polym. Sci.*, 2019, **37**, 383–393; (j) Q. Li and Z. Li, *Sci. China Mater.*, 2019, DOI: 10.1007/s40843-019-1172-2; (k) X. Chen, W. Luo, H. Ma, Q. Peng, W. Yuan and Y. Zhang, *Sci. China: Chem.*, 2018, **61**, 351–359.



- 4 (a) Z. An, C. Zheng, Y. Tao, R. Chen, H. Shi, T. Chen, Z. Wang, H. Li, R. Deng, X. Liu and W. Huang, *Nat. Mater.*, 2015, **14**, 685–690; (b) L. Gu, H. Shi, L. Bian, M. Gu, K. Ling, X. Wang, H. Ma, S. Cai, W. Ning, L. Fu, H. Wang, S. Wang, Y. Gao, W. Yao, F. Huo, Y. Tao, Z. An, X. Liu and W. Huang, *Nat. Photonics*, 2019, **13**, 373–375; (c) Z. Yang, Z. Mao, X. Zhang, D. Ou, Y. Mu, Y. Zhang, C. Zhao, S. Liu, Z. Chi, J. Xu, Y. Wu, P. Lu, A. Lien and M. R. Bryce, *Angew. Chem., Int. Ed.*, 2016, **55**, 2181–2185; (d) J. Yang, X. Zhen, B. Wang, X. Gao, Z. Ren, J. Wang, Y. Xie, J. Li, Q. Peng, K. Pu and Z. Li, *Nat. Commun.*, 2018, **9**, 840; (e) J. Yang, H. Gao, Y. Wang, Y. Yu, Y. Gong, M. Fang, D. Ding, W. Hu, B. Z. Tang and Z. Li, *Mater. Chem. Front.*, 2019, **3**, 1391–1397; (f) X. Wang, H. Xiao, P. Chen, Q. Yang, B. Chen, C. Tung, Y. Chen and L. Wu, *J. Am. Chem. Soc.*, 2019, **141**, 5045–5050.
- 5 (a) Y. Wei, Z. Zhang, Y. Chen, C. Wu, Z. Liu, S. Ho, J. Liu, J. Lin and P. Chou, *Chem. Commun.*, 2019, **2**, 10; (b) M. Yuan, D. Wang, P. Xue, W. Wang, J. Wang, Q. Tu, Z. Liu, Y. Liu, Y. Zhang and J. Wang, *Chem. Mater.*, 2014, **26**, 2467–2477.
- 6 (a) H. Uoyama, K. Goushi, K. Shizu, H. Nomura and C. Adachi, *Nature*, 2012, **492**, 234–238; (b) Y. Wada, S. Kubo and H. Kaji, *Adv. Mater.*, 2018, 1705641; (c) D. M. E. Freeman, A. J. Musser, J. M. Frost, H. L. Stern, A. K. Forster, K. J. Fallon, A. G. Rapisarda, F. Cacialli, I. McCulloch, T. M. Clarke, R. H. Friend and H. Bronstein, *J. Am. Chem. Soc.*, 2017, **139**, 11073–11080; (d) Y. Im, M. Kim, Y. J. Cho, J. Seo, K. S. Yook and J. Y. Lee, *Chem. Mater.*, 2017, **29**, 1946–1963; (e) I. S. Park, H. Komiyama and T. Yasuda, *Chem. Sci.*, 2017, **8**, 953–960; (f) Y. Kondo, K. Yoshiura, S. Kitera, H. Nishi, S. Oda, H. Gotoh, Y. Sasada, M. Yanai and T. Hatakeyama, *Nat. Photonics*, 2019, **13**, 678–682; (g) N. B. Kotadiya, P. W. M. Blom and G. A. H. Wetzelaer, *Nat. Photonics*, 2019, **13**, 765–769.
- 7 (a) S. Tian, H. Ma, X. Wang, A. Lv, H. Shi, Y. Geng, J. Li, F. Liang, Z. Su, Z. An and W. Huang, *Angew. Chem., Int. Ed.*, 2019, **58**, 6645–6649; (b) Y. Gong, L. Zhao, Q. Peng, D. Fan, W. Yuan, Y. Zhang and B. Z. Tang, *Chem. Sci.*, 2015, **6**, 4438–4444.
- 8 Y. Gong, P. Zhang, Y. Gu, J. Wang, M. Han, C. Chen, X. Zhan, Z. Xie, B. Zou, Q. Peng, Z. Chi and Z. Li, *Adv. Opt. Mater.*, 2018, **6**, 1800198.
- 9 (a) Z. Yang, Z. Mao, Z. Xie, Y. Zhang, S. Liu, J. Zhao, J. Xu, Z. Chi and M. P. Aldred, *Chem. Soc. Rev.*, 2017, **46**, 915–1016; (b) T. Huang, W. Jiang and L. Duan, *J. Mater. Chem. C*, 2018, **6**, 5577–5596; (c) M. Aydemir, *Polym. Bull.*, 2019, **76**, 6429–6436; (d) T. Wang, X. Hua, Y. Yu, Y. Yuan, M. Fung and Z. Jiang, *Chin. J. Org. Chem.*, 2019, **39**, 1436–1443; (e) Z. Wang, J. Cai, M. Zhang, C. Zheng and B. Ji, *Acta Chim. Sin.*, 2019, **77**, 263–268.
- 10 S. Cai, H. Shi, Z. Zhang, X. Wang, H. Ma, N. Gan, Q. Wu, Z. Cheng, K. Ling, M. Gu, C. Ma, L. Gu, Z. An and W. Huang, *Angew. Chem., Int. Ed.*, 2018, **57**, 4005–4009.

